Element distribution in porous Ga oxide obtained by anodizing Ga in phosphoric acid

Toshiaki Kondo[1,z], Hisato Matsuya[2], Hiroki Habazaki[3]

[1]Department of Mechanical Systems Engineering, Aichi University of Technology, 50-2 Manori Nishihasama-cho, Gamagori, Aichi 443-0047, Japan

[2]Graduate School of Chemical Sciences and Engineering, Hokkaido University, Kita 13, Nishi 8, Kita-ku, Sapporo, Hokkaido 060-0808, Japan

[3]Division of Applied Chemistry, Faculty of Engineering, Hokkaido University, Kita 13, Nishi 8, Kita-ku, Sapporo, Hokkaido 060-0808, Japan

[z]Corresponding Author E-mail Address: kondo-toshiaki@aut.ac.jp

Abstract

A STEM/EDS study of a porous Ga oxide film formed by an anodization process was conducted in this study to examine the crystalline structure of the film and the elemental distribution in the oxide film before and after heat treatment. The as-formed anodic film with a morphology resembling the well-known porous anodic Al oxide film was amorphous, crystallizing after heat treatment at 600 °C without changing the morphology and elemental distribution. The EDS elemental maps disclosed the duplex nature of the pore wall oxide; the phosphate anion was contaminated in the outer oxide layer next to the pores, and the inner layer consisted of relatively pure Ga oxide, practically free from phosphate. The similarity of morphology and elemental distributions between the porous anodic Al and Ga oxides suggests that the growth of both anodic oxide films proceeds under the same mechanism. In addition, crystallized porous Ga oxides are expected to be applied to fabricate various functional devices requiring geometrically controlled semiconductor nanohole arrays, such as devices for hydrogen formation.

Introduction

Porous Ga oxides, which have a nanohole array architecture, have attracted attention owing to their large surface area and semiconductor properties suitable for water splitting. Therefore, these porous Ga oxides are expected to be applied to devices for hydrogen formation based on water splitting [1,2]. The performance of such devices depends on the geometrical structures and semiconductor properties of the porous Ga oxide, and the semiconductor properties depend on the material composition of the Ga oxide. Therefore, to improve the device performance, the control of the geometrical structures and material compositions of porous Ga oxide is important. To date, various fabrication processes for Ga oxide, such as mist chemical vapor deposition (CVD) method and halide vapor phase epitaxy (HVPE) method, have been proposed [3,4]. These processes enable the formation of a crystalline Ga oxide layer on a substrate. However, these processes are unsuitable for preparing a Ga oxide layer with complex geometrical structures, such as a nanohole array structure, because these processes are intrinsically suitable for preparing a smooth film. As a fabrication process for porous Ga oxide layers, the anodization process has recently attracted considerable attention because it is suitable for the mass production of nanohole array structures. In this anodization process, a porous Ga oxide layer is formed on the surface of a Ga plate by applying a voltage between the Ga plate and the counter electrode in an acidic electrolyte [1,2,5]. However, until now, there are only a few reports about anodizing Ga plates because of the difficulties in handling Ga metal owing to its low melting point of 30 ˚C. Our group has reported a fabrication process for a geometrically controlled porous Ga oxide layer based on the anodization process at 0 ˚C [6]. The performance of water-splitting

devices based on a porous Ga oxide also depends on the spatial distribution and type of dopant in the porous Ga oxide. Schmuki et al. reported that Zn could be doped to a porous Ga oxide by anodizing a Zn–Ga alloy [1]. They also reported that phosphate anions were incorporated from a phosphoric acid electrolyte into the porous Ga oxide during anodization. They observed that dopants helped improve the efficiency of hydrogen formation. The incorporation of anions from the anodization electrolyte into a semiconductor porous oxide layer, such as anodic porous titania, has been studied in detail [7,8]. The anions incorporated into the porous titania act as dopants. The dopants generate a new energy level above the valance band of the titania; as a result, the bandgap of the titania is narrowed down [9–12]. Although pure titania responds only to ultraviolet light, titania containing dopants responds to visible light, improving photocatalytic reaction efficiency. In addition, controlling the anion distribution in porous titania is important to improve the photocatalytic reaction efficiency. The anion distributions in anodic porous structures, such as anodic porous alumina, anodic porous titania, and anodic porous iron oxide, have been well investigated [13–17]. In porous titania, for instance, photoexcited carriers that have survived deactivation can migrate to the surfaces of nanohole walls and then induce water-splitting reactions. By decreasing the migration length, the deactivation of photoexcited carriers can be suppressed. The photoexcited carriers generated near the surface of a nanohole wall can easily reach the reaction sites and then efficiently contribute to water-splitting reactions. Therefore, the investigation of element distribution in an anodic porous structure is a considerable issue to apply an anodic porous structure to a photoelectrode. However, until now, the element distribution in a porous Ga oxide has not yet been clarified. In the present research, the

element distribution in a porous Ga oxide fabricated by anodization was studied to expand the application field of porous Ga oxides and understand the anodization mechanism of Ga.

Experimental

The fabrication process for a porous Ga oxide has been described in previous reports [6]. Here, the fabrication process is briefly explained. A Ga plate was prepared by cooling a liquid Ga placed between two acrylic plates using a Peltier device. A Ga plate was anodized in 1 M phosphoric acid solution at -2 ˚C by applying a 40–80 V for 30 min to 2 h. After anodization, the porous Ga oxide membrane was obtained by selectively dissolving part of Ga in a saturated I_2 methanol solution. The crystallization of the membrane was implemented by heat treatment. The samples were annealed in air at 600 ˚C for 3 h [1]. The geometrical structures of the samples were observed using a scanning electron microscope (SEM; JSM-7500F, JEOL Ltd.). The element distribution in the porous Ga oxide and the crystallinity of the Ga oxide were evaluated using a scanning transmitted electron microscope (STEM; Titan3 G2, FEI Company Japan Ltd.). Prior to STEM observations, the porous Ga oxide membrane was thinned using a precision ion polishing system (PIPS; Model 691, Gatan Inc.). For cross-sectional STEM observations, a thin sample was cut out from the membrane using a focused ion beam and SEM (FIB-SEM; JIB-4601F, JEOL Ltd.) system equipped with a liquid Ga ion source.

Results and Discussion

Figure 1(a) shows a schematic diagram of the porous Ga oxide formed on a Ga metal.

The straight nanohole is located at the center of each hexagonal columnar cell. At the bottom of each nanohole, there is a dome-like structure that is called a barrier layer. Figures 1(b)–(f) show typical SEM images of the obtained porous Ga oxide membrane. Figure 1(b) shows a frontal SEM image of the porous Ga oxide membrane. From the SEM image, the formation of the nanohole array was observed. The arrangement of the nanoholes was random. Figure 1(c) shows a SEM image of the barrier layer. The domain architecture consisting of ordered arrays of barrier layers was formed. It is considered that the nanoholes were automatically arranged during anodization. The diameter of a cell, equivalent to an interpore distance, was 320 nm. Figure 1(d) shows a cross-sectional low-magnification SEM image of the porous Ga oxide membrane. The thickness of the membrane was 27 μm. Figures 1(e) and (f) show cross-sectional high-magnification SEM images around the front and back sides of the membrane, respectively. From Fig. 1(e), the formation of straight nanoholes growing perpendicularly to the sample surface was observed. As shown in Fig. 1(f), although the deep nanoholes were formed, their straightness shape was maintained without branching. The thickness of the barrier layer was 90 nm. During anodization, the anions originating from the anodizing electrolyte are thought to be incorporated into the anodic oxide layer. The number of incorporated anions basically depends on the electric field intensity at the barrier layer [18]. The electric field intensity at the barrier layer could be simply estimated by dividing the anodizing voltage by the barrier layer thickness. In the present research, the electric field intensity was estimated to be 0.89×10^{9} V/m. It was almost similar to the case of the anodic porous alumina, which had been reported to be 0.77×10^{9} – 1.0×10^{9} V/m [19]. The anodic porous alumina is one of the most typical nanohole

arrays obtained by anodization. The incorporation of anions originating from the anodizing electrolyte into anodic porous alumina has been observed [13,14]. The incorporation of anions into a porous Ga oxide is likely to occur similarly to that into anodic porous alumina.

The element distribution in the porous Ga oxide was examined by STEM. Prior to STEM observations, the porous Ga oxide membrane was thinned using the PIPS. During thinning to ~200 nm, a sample was cooled to suppress thermal damage of the sample. Figure 2(a) shows a frontal high-angle annular dark-field (HAADF) image of the porous Ga oxide membrane. Each black circle represents a nanohole, which is located at the center of a hexagonal columnar cell. A cell boundary appeared brighter than other parts of the sample. This means that high-atomic-number elements are more abundant at the cell boundary than elsewhere. Figures 2(b)–(d) show the distributions of the Ga, O, and P elements measured by energy-dispersive X-ray spectroscopy (EDS). Figure 2(b) shows that Ga is distributed throughout the pore wall oxide, and the concentration of Ga is slightly high at the cell boundary. Figure 2(c) shows that O is homogenously distributed throughout the pore wall oxide. However, Fig. 2(d) reveals that the cell boundary is deficient in the P element. Figure 2(i) shows the concentration profile of P measured along the direction indicated by an arrow shown in Fig. 2(a). Regions 1 and 3 correspond to the outer oxide layer. The concentration of P was 3–4 %. Region 2 corresponds to the cell boundary (inner oxide layer). It can be confirmed that the concentration of P was low at the cell boundary.

We also examined a cross-sectional element distribution in a porous Ga oxide membrane. The FIB-SEM system was used to obtain an electron-transparent thin cross-section, ~200 nm

thick, from the porous Ga oxide membrane. Figure 2(e) shows a cross-sectional HAADF image of the porous Ga oxide membrane. The distributions of Ga, O, and P are shown in Figures 2(f)–(h). Both Ga and O distribute uniformly in the pore wall oxide, as shown in Figs. 2(f) and (g). The arrows shown in Fig. 2(h) indicate the positions of the cell boundaries. The concentration of P was low at the cell boundary along the hole depth direction, being consistent with Fig. 2(d). At the cell boundary, a high-purity Ga oxide practically free from P was expected to be formed. The element distribution in the porous Ga oxide tended to qualitatively agree with that in an anodic porous alumina formed by anodizing an Al plate in a phosphoric acid solution [13]. Therefore, the incorporation mechanism of anions into the porous Ga oxide is supposed to be similar to that into the anodic porous alumina. During anodization, phosphate anions originating from the anodizing electrolyte and O^{2-} or OH^- originating from water contained in the electrolyte were adsorbed on the barrier layer at the pore base and incorporated into the anodic Ga oxide under a high electric field. The negatively charged phosphate anions and O^{2-}/OH^- migrated toward the oxide/metal interface, with the migration of the phosphate anions slower than that of O^{2-}/OH^- [18,20]. Therefore, it is thought that the phosphate anions could not reach the oxide/metal interface, forming a low-P-concentration area at the cell boundary. In actuality, the migration behavior of the anions in the Ga oxide is thought not to be simple. Hebert et al. proposed the flow model for the formation of anodic porous alumina [21]. During the anodization of Al, the anions were transported in the anodic porous alumina by viscous flow in addition to the electrical migration. The viscous flow was induced in the porous alumina by compressive stress near the pore base. The compressive stress might be occurred by

several reasons, such as volume expansion due to the anodic oxidation, Maxwell stress, and electrostriction. The viscous flow is thought to occur during the formation of the porous Ga oxide as is the case in the anodic porous alumina. Figure 2(j) shows a selected area electron diffraction (SAED) pattern of an as-formed porous Ga oxide measured at the position encircled in white in Fig. 2(e). Only broad halo rings were observed, indicating that the obtained Ga oxide was amorphous.

The dependence of the anodizing voltage on an element distribution was investigated. A Ga plate was anodized by applying 40 V. Figure 3(a) shows a frontal HAADF image of the porous Ga oxide. The formation of the porous structure was confirmed even though the anodizing voltage was reduced to half. The diameter and interpore distance of the nanoholes in the porous Ga oxide, that were 180 and 220 nm, were reduced by reducing the anodizing voltage. Figures 3(b)–(d) show the distributions of the Ga, O, and P elements measured by EDS. The element distributions of Ga, O, and P are almost the same as that shown in Fig. 2(b)–(d). The P concentration at the pore wall oxide, which was 3–4 %, was unchanged despite the anodizing voltage being decreased by half.

To improve the reaction efficiency of water splitting on the porous Ga oxide, the crystallization of the porous Ga oxide will be required. In the present study, an attempt was made to crystallize the porous Ga oxide by annealing in air at 600 ˚C for 3 h. Figure 4(a) shows a photograph of the annealed porous Ga oxide membrane. Its shape remained unchanged, and no cracks were generated even after annealing at such a high temperature. The mechanical strength of the membrane seems not to be degraded. The membrane could be easily handled by hands and tweezers. Figures 4(b)–(d) show typical SEM images of the

annealed porous Ga oxide membrane. From these SEM images, the geometrical structures of the porous Ga oxide were confirmed to remain intact even after annealing.

Next, the element distribution in the annealed porous Ga oxide was investigated. Figures 5(a)–(e) show STEM observation results of the annealed porous Ga oxide membrane. Figure 5(a) shows a cross-sectional HAADF image of the annealed porous Ga oxide membrane. The cell boundary appears brighter than other parts, revealing that the high-atomic-number element, Ga, is abundant at the cell boundary. Figures 5(b)–(d) show the distributions of Ga, O, and P. Figures 5(b) and (c) show that Ga and O are distributed almost uniformly throughout the pore wall oxide; however, Fig. 5(d) discloses the deficiency of P at the cell boundary. These results show that the element distribution in the anodic porous Ga oxide remained the same even after the thermal crystallization of Ga oxide. Crystallization of oxide was confirmed by a SAED pattern shown in Fig. 5(e). The SAED pattern shows many diffraction spots, which indicate the presence of β-Ga_2O_3 phase. A diffuse halo also remained, suggesting that a part of the oxide, probably a phosphate-containing oxide, was not fully crystallized [22–24].

Conclusions

The porous Ga oxide was obtained by anodizing a Ga plate in the phosphoric acid solution. The element distribution in the anodic porous Ga oxide was investigated by STEM. Ga and O were distributed relatively uniformly throughout the pore wall oxide. It was observed that the concentration of Ga was slightly high at the cell boundary of the porous Ga oxide membrane. In contrast, the P concentration was low at the cell boundary. During

anodization, the phosphate anions and O^{2-}/OH^- originating from the electrolyte were incorporated into the Ga oxide at the barrier layers under a high electric field. The incorporated phosphate anions and O^{2-}/OH^- migrated toward the oxide/metal interface, but the phosphate anions could not reach the interface because their migration was thought to be slower than that of O^{2-}/OH^-. The as-formed porous Ga oxide, which was amorphous, could be crystallized by heat treatment at 600 ˚C. The element distribution in the porous Ga oxide remained the same even after annealing. In addition, the crystallized porous Ga membrane still maintained its high mechanical strength. The crystallized porous Ga oxide membrane is expected to be applied to various functional devices requiring geometrically controlled semiconductor nanohole arrays, such as hydrogen-forming devices and functional ultraprecise filters.

Acknowledgments

This work was supported by JSPS KAKENHI Grant Number JP22K05272. Part of this work was supported by the "Advanced Research Infrastructure for Materials and Nanotechnology in Japan (ARIM)" of the Ministry of Education, Culture, Sports, Science and Technology (MEXT), and by Grant Number JPMXP1222NU0401. We thank Mr. Ikuo Hayashi of ARIM at Nagoya University for his great technical support in SEM observation. Part of this work was supported by the Joint Usage/Research Center for Catalysis at Hokkaido University and by Proposal Number 22DS0128. Part of this work was conducted at "Joint-Use Facilities: Laboratory of Nano-Micro Material Analysis" at Hokkaido University, supported by ARIM of MEXT and by Proposal Number JPMXP1222HK0022.

We thank Mr. Kenji Ohkubo and Mr. Ryo Ota of the Technical Center of Engineering at Hokkaido University for their great technical support in sample preparations by PIPS and STEM observations, respectively. We thank Mr. Atsuki Sawa of the Technical Center of Engineering at Hokkaido University for his great technical support in sample preparations using the FIB-SEM system.

References

1. N. K. Shrestha, K. Lee, R. Kirchgeorg, R. Hahn, P. Schmuki, *Electrochem. Commun.*, **35**, 112–115 (2013).
2. N. K. Schrestha, H. T. Bui, T. Lee, Y.-Y. Noh, *Langmuir*, **34**, 4575–4583 (2018).
3. M. Higashiwaki, K. Sasaki, A. Kuramata, T. Masui, S. Yamakoshi, *Phys. Status Solidi A*, **211**, 21–26 (2014).
4. K. Goto, K. Konishi, H. Murakami, Y. Kumagai, B. Monemar, M. Higashiwaki, A. Kuramata, S. Yamakoshi, *Thin Solid Films*, **666**, 182–184 (2018).
5. B. Pandey, P. S. Thapa, D. A. Higgins, T. Ito, *Langmuir*, **28**, 13705–13711 (2012).
6. T. Kondo, Y. Kuroda, T. Shichijo, T. Yanagishita, H. Masuda, *J. Vac. Sci. Technol. B*, **40**, 010603 (2022).
7. J. M. Macak, L. V. Taveira, H. Tsuchiya, K. Sirotna, J. Macak, P. Schmuki, *J. Electroceram.*, **16**, 29–34 (2006).
8. J. M. Macak, H. Tsuchiya, A. Ghicov, K. Yasuda, R. Hahn, S. Bauer, P. Schmuki, *Curr. Opin. Solid State Mater. Sci.*, **11**, 3–18 (2007).
9. Y.-C. Nah, I. Paramasivam, P. Schmuki, *ChemPhysChem*, **11**, 2698–2713 (2010).
10. D. He, Y. Li, I. Wang, J. Wu, Y. Yang, Q. An, *Appl. Surf. Sci.*, **391**, 318–325 (2017).
11. R. P. Antony, T. Mathews, P.K. Ajikumar, D. N. Krishna, S. Dash, A.K. Tyagi, *Mater. Res. Bull.*, **47**, 4491–4497 (2012).
12. R. Asahi, T. Morikawa, T. Ohwaki, K. Aoki, Y. Taga, *Science*, 293, 269–271 (2001).
13. F. Le Coz, L. Arurault, L Datas, *Mater. Charact.*, **61**, 283–288 (2010).
14. G. E. Thompson, R. C. Fumeaux, G. C. Wood, *J. Electrochem. Soc.*, **125**, 1480–1482

(1978).

15. S. P. Albu, A. Ghicov, S. Aldabergenova, P. Drechsel, D. LeClere, G. E. Thompson, J. M. Macak, P. Schmuki, *Adv. Mater.*, **20**, 4135–4139 (2008).
16. K. Shahzad, D. Kowalski, C. Zhu, Y. Aoki, H. Habazaki, *ChemElectroChem*, **5**, 610–618 (2018).
17. A. M. Brudzisz, D. Giziński, W. J. Stępniowski, *Molecules*, **26**, 6378 (2021).
18. H. Takahashi, F. Fujimoto, H. Konno, M. Nagayama, *J. Electrochem. Soc.*, **131**, 1856–1861 (1984).
19. M. S. Hunter, P. Fowle, *J. Electrochem. Soc.*, 101, 481–485 (1954).
20. G. C. Wood, P. Skeldon, G. E. Thompson, K. Shimizu, *J. Electrochem. Soc.*, **143**, 74–83 (1996).
21. J. E. Houser, K. R. Hebert, *Nat. Mater.*, **8**, 415-420 (2009).
22. K. Shimizu, G. E. Thompson, G. C. Wood, *Thin Solid Films*, **77**, 313-318 (1981).
23. K. Shimizu, G. E. Thompson, G. C. Wood, *Thin Solid Films*, **81**, 39-44 (1981).
24. H. Hashimoto, Y. Fujita, K. Yazawa, H. Asoh, *J. Phys. Chem. Solids*, **178**, 111312 (2023).

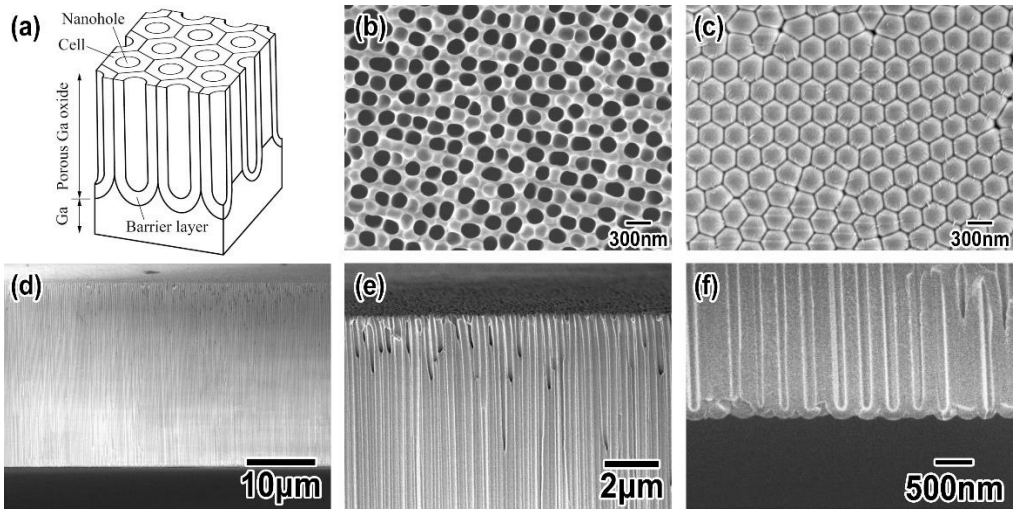

Figure 1 (a) Schematic of porous Ga oxide obtained by anodization. Each nanohole is located at the center of a hexagonal columnar cell. The bottom part of the cell is called a barrier layer. (b) Front- and (c) back-side SEM images of the porous Ga oxide membrane. (d) Cross-sectional low-magnification SEM image of the membrane. (e), (f) Cross-sectional high-magnification SEM images around front and back sides of the membrane, respectively. The porous Ga oxide was formed by anodizing a Ga plate in 1 M phosphoric acid solution at -2 °C by applying a voltage of 80 V for 1 h. Part of Ga was selectively dissolved by wet etching.

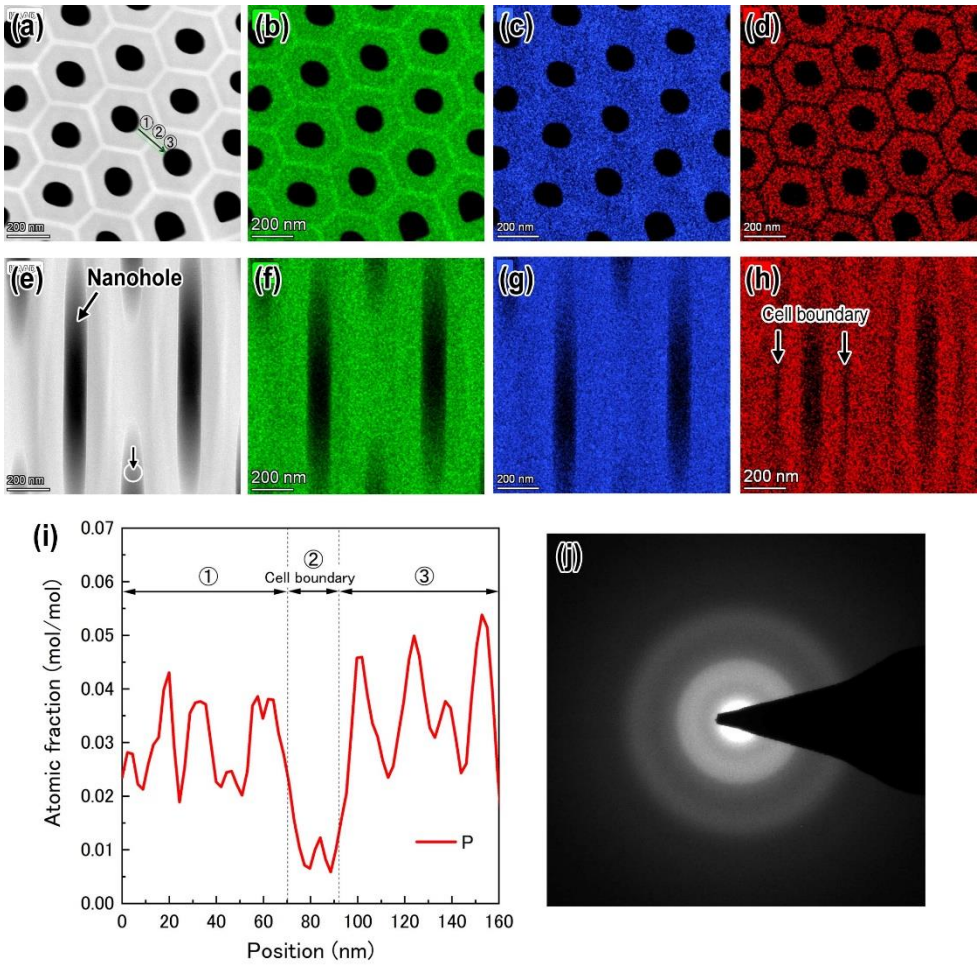

Figure 2 (a) Frontal HAADF image of the porous Ga oxide which was obtained by applying 80 V to a Ga plate. (b)–(d) Frontal EDS mapping images of (b) Ga, (c) O, and (d) P. (e) Cross-sectional HAADF image of the porous Ga oxide. (f)–(h) Cross-sectional EDS mapping images of (f) Ga, (g) O, and (h) P. (i) Atomic fraction profile of P along the direction indicated by the arrow in (a). (j) SAED pattern measured at the position encircled in white in (e).

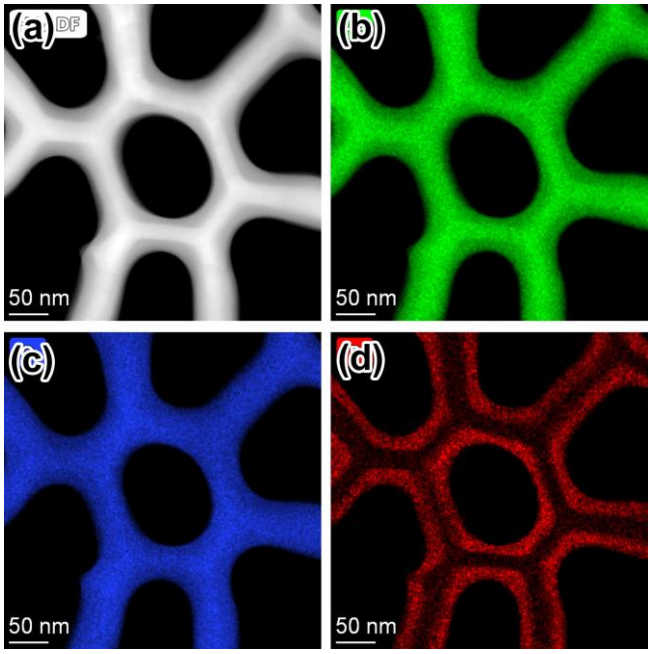

Figure 3 (a) Frontal HAADF image of the porous Ga oxide obtained by applying 40 V to a Ga plate for 2 h. (b)–(d) Frontal EDS mapping images of (b) Ga, (c) O, and (d) P.

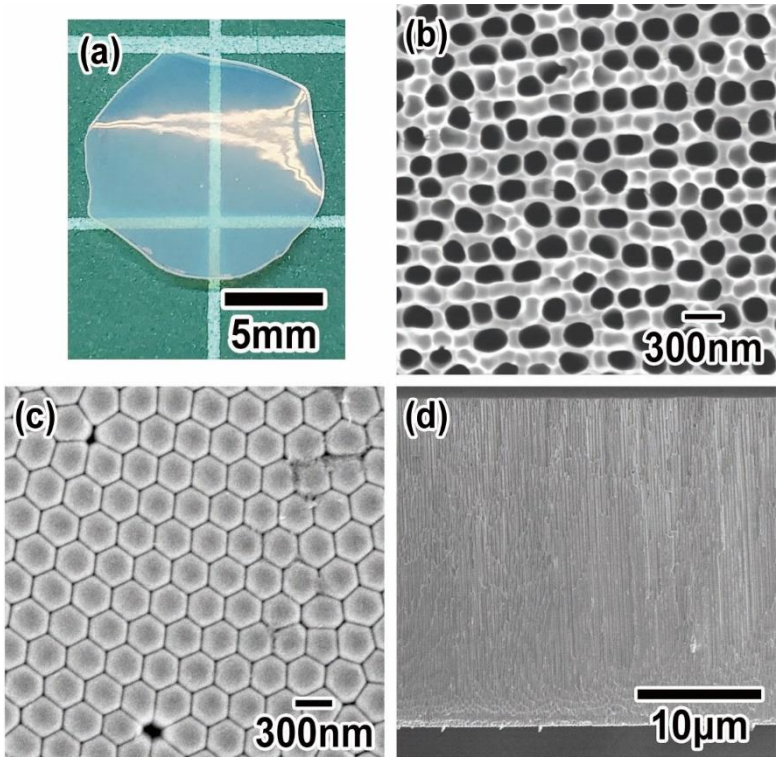

Figure 4　(a) Photograph of the porous Ga oxide membrane after annealing in air at 600 ˚C for 3 h.　(b) Frontal, (c) back-side, and (d) cross-sectional SEM images of the annealed porous Ga oxide membrane.

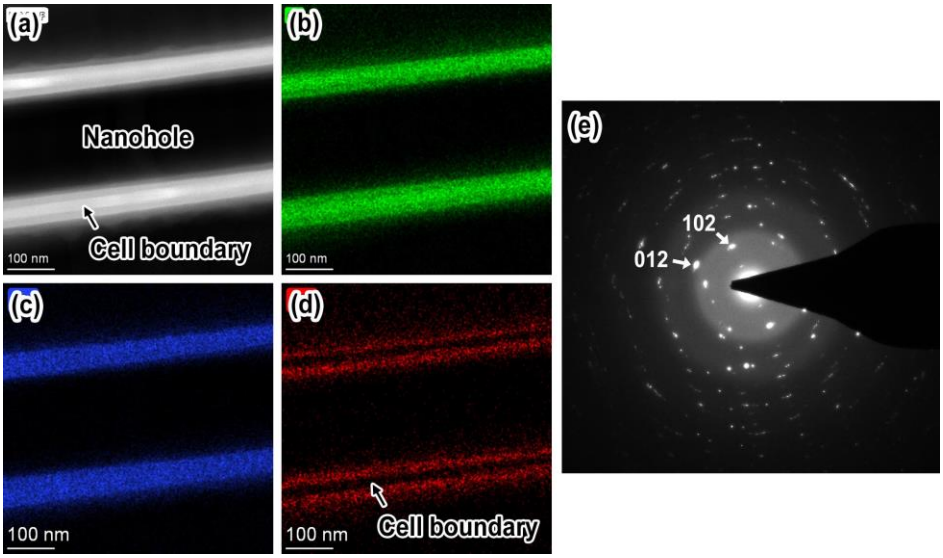

Figure 5 (a) Cross-sectional HAADF image of the annealed porous Ga oxide membrane. (b)–(d) EDS mapping images of (b) Ga, (c) O, and (d) P. (e) SAED pattern of the annealed membrane.